Desalination and Water Treatment
www.deswater.com

doi: 10.1080/19443994.2015.1009172

57 (2016) 6393–6400
March

Taylor & Francis
Taylor & Francis Group

Comparison of azo dye AR88 degradation efficiency using various oxidant systems

Danni Yang, Yitian Liu, Juan Mo, Xia Jiang, Zhishan Yang*

College of Architecture and Environment, Sichuan University, Chengdu 610065, P.R. China, Tel. +86 134 0847 9499; email: zyangdanni@sina.com (D. Yang), Tel. +86 187 2848 4280; email: liuyitianyiliu@163.com (Y. Liu), Tel. +86 151 9663 2496; email: mojuan2014@163.com (J. Mo), Tel. +86 136 8833 0205; email: xjiang@scu.edu.cn (X. Jiang), Tel. +86 28 8540 1682; Fax: +86 28 8540 3016; email: yangzs@scu.edu.cn (Z. Yang)

Received 20 April 2014; Accepted 13 January 2015

ABSTRACT

The degradation and mineralization of azo dyes, Acid Red 88 (AR88), were studied by several oxidant methods, including UV, H_2O_2, O_3, UV/O_3, UV/H_2O_2, O_3/H_2O_2, and UV/O_3/H_2O_2, and the production yields of the hydroxyl radicals (•OH) in each oxidation process were also determined. The results showed it could not produce a perceptible of •OH using single UV, H_2O_2, or O_3 method; however, the combined ones involving O_3, i.e. O_3/H_2O_2, UV/O_3, UV/O_3/H_2O_2, all showed high generation of •OH, which resulted in good degradation performance of AR88. Among the seven oxidation methods, UV/O_3/H_2O_2 was proved to be the best for generation of •OH with an average generation rate up to 1.13 mg L^{-1} min^{-1} in 30 min and also the most effective system for degradation and mineralization of AR88 with a total organic carbon (TOC) removal efficiency of 88% in 30 min after reaction. It was found that the pH value decreased as the increase of TOC and AR88 removal efficiencies during the mineralization process. The degradation intermediates including benzene, naphthalene, naphthalene sulfonic acid, and phthalic acid were detected using gas chromatography–mass spectrometry.

Keywords: Hydroxyl radicals; O_3; Acid Red 88; Advanced oxidation processes

1. Introduction

As the largest class of dyes used in textile, leather, and paper industries [1], azo dyes are very stable with good resistance to sunlight and aerobic degradation. When Acid Red 88 (AR88) solution is incorporated into the body, they can be cleaved into aromatic amines which are toxic, carcinogenic, and mutagenic [2,3]. It is estimated that approximately 2% of the total synthetic dyes produced worldwide are lost directly during the dyeing process, and 10% are subsequently discharged in the textile effluents during the coloration process [4]. Therefore, the elimination of hazardous dyes from textile wastewater effluents is vital for human beings [5]. But the wastewater discharged from textile industry is hard to be degraded by conventional methods due to its high toxicity, complicated compounds, and biological hazard. Other methods like biodegradation and chemical precipitation have been used for the removal of certain dyes. However, biodegradation process is always accompanied by the formation of carcinogenic and toxic by-products [6], while chemical precipitation method generates problems in sludge handling and disposal [7]. In order to

---

*Corresponding author.

overcome these limitations, it is necessary to adopt reactive systems, which are much more effective than the conventional ones.

In recent years, the systems of O_3, H_2O_2, UV, and combinations of various processes, which can generate numerous hydroxyl radicals within a short time, have been widely used in the degradation and complete mineralization of azo dyes because of its exceptional properties such as low cost, simple process, efficient oxidation, nontoxicity, and no dangerous by-products. Hydroxyl radical is an extraordinarily reactive species which can attack most parts of the organic molecules at a rapid rate [8]. Many researchers have used AOPs for photocatalysis, sonolysis, Fenton and modified Fenton reactions, ozonation, and UV/H_2O_2 for the degradation of azo dyes [9–13]. Matilainen and Sillanpää [14] provided a thorough review of published oxidation and AOPs studies that have been conducted on both industrial and synthetic wastewaters. However, these studies were primarily focused on evaluating the post-process determination of residuals or the effects of various parameters on removal performance [15].

In this study, the yields of •OH generated in the UV, H_2O_2, O_3, and combinations of various systems were determined to compare their oxidation capacities directly and the degradation efficiencies of AR88 by various oxidation systems were also compared in parallel. In addition, gas chromatography–mass spectrometer (GC-MS) was used to detect the intermediate products of AR88 degradation.

2. Materials and methods

2.1. Materials

Dimethyl sulfoxide (DMSO, reagent pure grade), 2, 4-initrobenzene hydrazine (DNPH, reagent pure grade), formaldehyde (37–38 wt.%), and hydrogen peroxide (30 wt.%) were obtained from Sigma-Aldrich. Phosphoric acid (85%) and sodium dihydrogen phosphate were analytical grade reagents purchased from Fisher Scientific. AR88 ($C_{20}H_{13}N_2O_4SNa$) was obtained from Sinopharm (dye content 99%), which absorbs in the visible region ($\lambda_{max} = 506$ nm; $\varepsilon_{506} = 1.55 \times 10^4\ M^{-1}\ cm^{-1}$). It is an azo dye bearing two sulfonic groups as presented in Fig. 1. The desired concentration of AR88 was prepared from the stock solution using Milli-Q water. All chemicals were used without further purification.

2.2. Experimental setup

The experimental reaction system includes an ozone generator, UV lamp, quartz sleeve, contactor (reactor), and off-gas collection system, as shown in Fig. 2. The ozone generator was obtained from Viresco Singapore Pincte Ltd, and it can produce ozone at a rate of $190 \pm 8.3\ mg\ h^{-1}$. A low pressure 15 w UV lamp (Qidong Fluorescent Lamp Factory, China) with 253.7 nm wavelength was utilized as the radiation source. The UV lamp was preheated for 5 min before each use. The light intensity of the UV lamp was $77{,}200 \pm 600\ mw/m^2$ which was determined at a distance of 1 cm using a VECTOR H410 radiometer (Scientech Boulder Co. USA, Model No, AC5000). The UV lamp was held in a quartz tube (O.D. 4 cm). The quartz tube was placed at the center of the reactor to provide UV radiation for the reaction mixture. The reactor was made of glass with a volume of about 1 L (6 cm diameter × 35 cm height). A quartz diffuser placed at the bottom of the reactor produced a myriad of tiny air bubbles in order to increase the gas–liquid contact area and improve the mass transfer efficiency. The ozone generated from the ozone generator was sent into the base of the reactor through silicone tubing. Water samples were taken from the middle part of the reactor. A potassium iodide solution (2%) was used to collect the residual ozone from the off-gas from the reactor. Silicone tubing was used for all connections between the ozone generator and the reaction vessel.

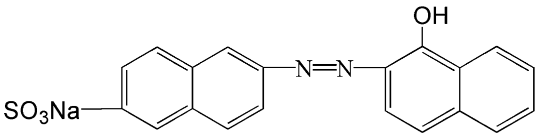

Fig. 1. Structure of Acid Red 88.

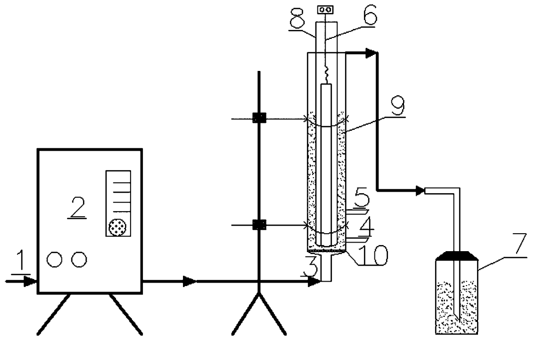

Fig. 2. Schematic diagram of reactor system: (1) air inlet; (2) ozonizer; (3) inlet of ozone; (4) drain line; (5) sampling point; (6) UV lamp; (7) ozone killer; (8) quartz tube; (9) reactor chamber; (10) porous plate.

For the degradation of AR88, aqueous solutions containing AR88 with a concentration of 25 mg L^{-1} were prepared with Milli-Q water. About 250 mL of the AR88 solution was placed in the reactor vessel to be treated by •OH radicals generated from various AOPs systems. For all experiments involving H_2O_2, 20 mg L^{-1} of hydrogen peroxide solution was added. The initial total organic carbon (TOC) and pH of the AR88 solution were 12.20 ± 0.27 mg L^{-1} and 6.2 ± 0.2, respectively. Samples were drawn from the reactor vessel at regular intervals for analysis. All the experiments were performed at room temperature (about 25℃).

2.3. Analytical methods

The dimethyl sulfoxide trapping method developed by Chao et al. [16] was used to determine the yield of hydroxyl radicals generated in AOPs, including UV, H_2O_2, O_3, UV/O_3, UV/H_2O_2, O_3/H_2O_2, and UV/O_3/H_2O_2. The method employed the reaction between hydroxyl radicals and DMSO to generate quantitatively formaldehyde, which then reacted with DNPH to form the corresponding hydrazone (HCHO-DNPH) to be analyzed by High Performance Liquid Chromatography (HPLC, WATERS 2695). About 5 mL of samples were taken from the bottom of the reactor at specified time intervals, and 1 mL of 0.5 mol L^{-1} H_3PO_4-NaH_2PO_4 buffer solution (pH 4.0) and 0.3 mL of 6 mmol L^{-1} DNPH solution were mixed with formaldehyde. The mixture was maintained at room temperature for 30 min and then analyzed by HPLC. Water–acetonitrile–carboxylic acid (acetonitrile:water:50 mM formic acid = 40:50:10) was used as the mobile phase in the HPLC analysis and the flow rate was set at 1.0 mL/min. The detection wavelength was 254 nm.

In this study, the degradation efficiency of each treatment process was evaluated by determining the concentration of AR88 using a spectrophotometer (UV–vis Spectrophotometer Jasco V-550) at λ_{max} = 506 nm, and the mineralization of AR88 was evaluated by TOC analysis using a Shimadzu TOC-Vcph analyzer after the samples filtered through a 0.45 μm PTFE filter. GC-MS (QP2010Plus Shimdzu) was used for analyzing the intermediate degradation products. An AR88 solution of 25 mg L^{-1} was treated by the UV/H_2O_2/O_3 system, and then a 20 mL of sample was extracted using 10 mL of CH_2Cl_2 (Chromatogram Pure Grade). 1 μL of sample was injected into a GC-MS system equipped with a HP-1MS capillary column (30 m × 0.32 m × 0.25 μm). A mass spectrometry detector with an electron ionization source (70 eV) was used and its ion source temperature was 200℃. The carrier gas flow rate of helium was set at 1.0 mL/min with an injection temperature of 100℃ and splitless mode was chosen during the treatment. The GC column was operated in temperature programed mode and the temperature was initially at 40℃ for 2 min, and increased at 10℃ min^{-1} to 120℃ (held for 5 min), then rise at 5℃ min^{-1} to 220℃ (held for 2 min), and finally reached at 20℃ min^{-1} to 280℃ (held for 10 min). Analysis was undertaken with reference to the NIST 05 mass spectral library database.

3. Results and discussion

3.1. The generation of hydroxyl radicals by AOPs systems

The generation of •OH in different systems were shown in Fig. 3. As ozone was constantly bubbled into the reactor of a continuous UV radiation, a nearly linear increase in •OH concentrations was observed at the time. Similar phenomena were also observed in other studies [16,17]. The seven oxidation processes were ranked in terms of •OH formation rate as follows: $H_2O_2 \approx UV < O_3 < O_3/H_2O_2 < UV/O_3 < UV/H_2O_2 < UV/O_3/H_2O_2$.

For the three single systems, •OH was not generated in the single UV or H_2O_2 system, while only a small amount of •OH was generated in the O_3 system with a generation rate of 0.17 mg L^{-1} min^{-1}. The O_3 is unstable and easy to decompose in aqueous solutions. It has been generally agreed that •OH is formed by the catalytic reaction between ozone and hydroxide ions, thus the ozone decomposition rate increased as solution pH value increases [18]. The decomposition

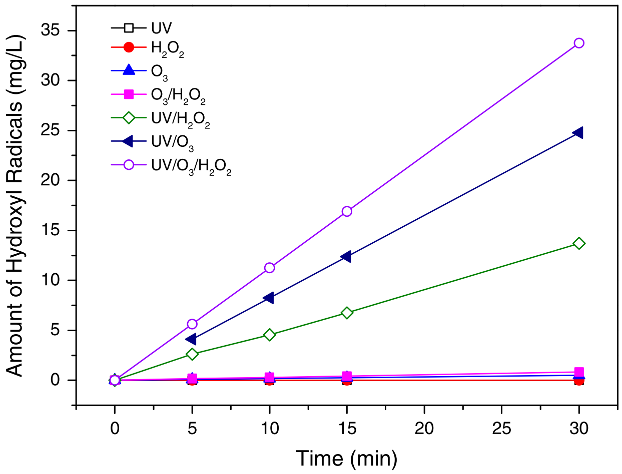

Fig. 3. Generation of hydroxyl radicals by different systems. DMSO: 0.5 mol/L, O_3: 3.17 mg/min, H_2O_2: 20 mg/L, the generation of hydroxyl radicals by UV/H_2O_2, UV/O_3, and UV/O_3/H_2O_2 were carried out under a 15 W ultraviolet lamp.

of ozone in aqueous solutions can be described as follows:

$$2\mathrm{O}_3 + \mathrm{H}_2\mathrm{O} \overset{\mathrm{OH}^-}{\rightarrow} \bullet\mathrm{OH} + 2\mathrm{O}_2 + \bullet\mathrm{HO}_2 \tag{1}$$

A DMSO solution with a neutral, or slightly acidic pH was used to trap •OH in this experiment, so the decomposition rate of O_3 in the aqueous solution was low, explaining why •OH radicals had a low production in the single O_3 system.

Although H_2O_2 was partly dissociated in the solution, it could be broken down into HO_2^- instead of •OH radicals as follows:

$$\mathrm{H}_2\mathrm{O}_2 + \mathrm{H}_2\mathrm{O} \rightarrow \mathrm{HO}_2^- + \mathrm{H}_3\mathrm{O}^+ \tag{2}$$

The UV irradiation (253.7 nm) corresponds to the photon energy of 4.88 eV which is less than the bond dissociation energy of O=O double bond in a solution (5.12 eV) and H–OH single bond of a water molecule (5.21 eV) [19]. Therefore, the UV radiation at 253.7 nm does not have sufficient energy to break the oxygen molecules or water molecules into •OH without the addition of an oxidant or catalyst. Only under UV radiation, with wavelengths less than 243 nm, the water molecules can be dissociated into hydrogen atoms and hydroxyl radicals,

$$\mathrm{H}_2\mathrm{O} + hv \overset{\lambda \leq 243\ \mathrm{nm}}{\rightarrow} \bullet\mathrm{OH} + \bullet\mathrm{H} \tag{3}$$

The UV irradiation can induce the homolytic cleavage of hydrogen peroxide to generate hydroxyl radicals [20]. The UV/H_2O_2 system showed a generation rate of •OH at $0.46\ \mathrm{mg\ L^{-1}\ min^{-1}}$ in 30 min, which was greater than the one in $UV/Fe^{2+}/H_2O_2$ system evaluated in other study [16]. In aqueous solutions, H_2O_2 is a scavenger of •OH which always lowers its yield in high H_2O_2 concentrations since H_2O_2 itself is attacked by •OH with a constant rate of $(2.7 \pm 0.3) \times 10^7\ \mathrm{M^{-1}\ s^{-1}}$ [21],

$$2(\mathrm{H}_2\mathrm{O}_2 + \bullet\mathrm{OH}) \rightarrow \mathrm{H}_2\mathrm{O} + \bullet\mathrm{HO}_2 \tag{4}$$

$$2 \bullet \mathrm{HO}_2 \longrightarrow \mathrm{H}_2\mathrm{O}_2 + \mathrm{O}_2 \tag{5}$$

The combined systems involving O_3, i.e. O_3/H_2O_2, UV/O_3, $UV/O_3/H_2O_2$, all showed a higher generation of •OH than that of single O_3 system. The average generation rates of •OH in 30 min were 0.27 and $0.83\ \mathrm{mg\ L^{-1}\ min^{-1}}$ in O_3/H_2O_2 and UV/O_3 systems, respectively. It was reported that the addition of H_2O_2 to the aqueous O_3 solution [22] or irradiation with UV light wavelength of 254 nm [23] would result in higher rates of •OH production. The extinction coefficient of O_3 at 254 nm was $3{,}600\ \mathrm{M^{-1}\ cm^{-1}}$, much higher than that of H_2O_2 [23], thus the UV/O_3 system had a higher generation rate of •OH than that of O_3/H_2O_2 system. In addition, $UV/O_3/H_2O_2$ is showed to be the best system for the generation of •OH, in which the average generation rate in 30 min could be up to $1.13\ \mathrm{mg\ L^{-1}\ min^{-1}}$. Other researchers evaluated the generation rate of •OH in heterogeneous photocatalytic process with Deguassa P25 TiO_2 catalysts [24] and the generation rate was determined to be $0.023\ \mathrm{mmol\ L^{-1}\ min^{-1}}$ (i.e. $0.39\ \mathrm{mg\ L^{-1}\ min^{-1}}$), much lower than that of $UV/O_3/H_2O_2$ system. This phenomenon was mainly resulted from the synergistic reaction between the O_3/H_2O_2 and H_2O_2/UV systems.

3.2. Degradation and mineralization of AR88 by AOPs

The AOP systems have been utilized for the treatment of AR88 by generating various reactive species such as radicals (•H, •O, $\bullet HO_2$) and molecular species (H_2O_2, O_3). The changes in concentrations of AR88 and TOC after each treatment process were determined to obtain degradation efficiencies and mineralization of AR88, as shown in Figs. 4 and 5. Generally speaking, the efficiency of AR88 degradation and TOC removal agreed with the generation rate of •OH in each treatment process. However, the TOC removal efficiencies of AR88 were lower than the degradation efficiencies of AR88 by these treatments because of the

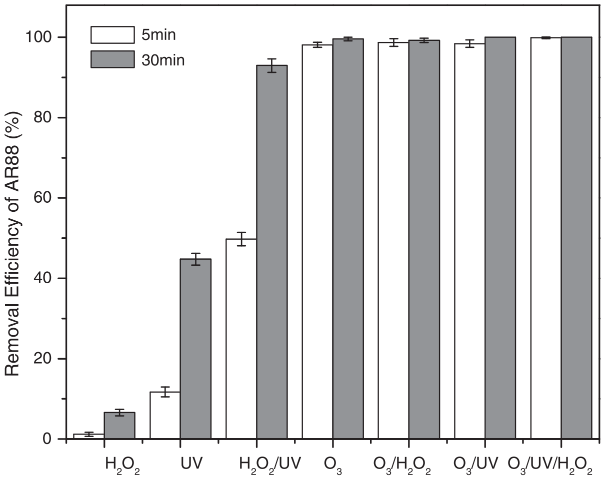

Fig. 4. The degradation efficiency of AR88 by the Seven oxidation processes (initial AR88 concentration: 25 mg/L; reaction volume: 250 mL; initial pH 6.2; H_2O_2 concentration: 20 mg/L).

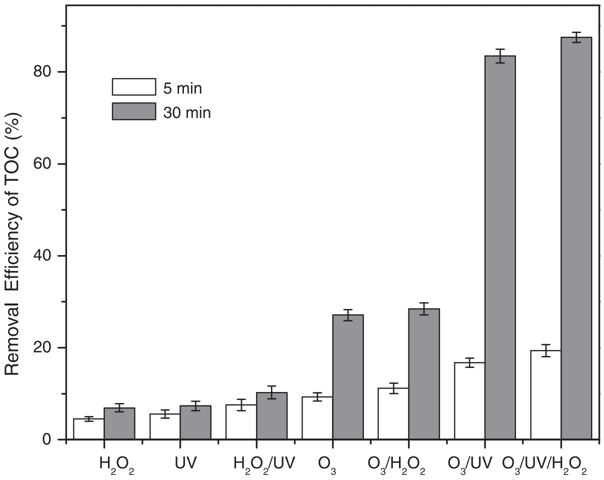

Fig. 5. Mineralization of AR88 by Seven oxidation processes (initial AR88 concentration: 25 mg/L; reaction volume: 250 mL; initial pH 6.2; H_2O_2 concentration: 20 mg/L).

partial oxidation of AR88 into other intermediate by-products. Previous studies reported that O_3 and •OH could attack the unsaturated double bond N=N, which was responsible for the characteristic color of the dye, via electrophilic substitution [17], while the cleavage of N=N bonds might not necessarily affect the carbon structure, and hence left the TOC concentration unaffected.

Single UV or H_2O_2 treatment had little impact on the degradation of AR88 and almost no impact on TOC removal. Other studies also observed a negligible impact upon natural organic matter (NOM) reduction by UV or H_2O_2 system alone [25]. When H_2O_2 was combined with UV, the rate of AR88 reduction increased significantly while no apparent increase was observed in the removal of TOC in the experiment. It was also shown that there was a significant removal of NOM without TOC reduction by H_2O_2/UV system with a UV at 254 nm at the dose of 1,500 mJ cm^{-2} and H_2O_2 concentrations at up to 20 mg L^{-1} [26]. Although the UV/H_2O_2 system had high •OH production (Fig. 3), the removal efficiencies of AR88 and TOC were lower after 5 min of treatment. This was due to the small molar extinction coefficient of H_2O_2, 18.6 M^{-1} cm^{-1} at 254 nm, and only a relative small fraction of incident light was therefore exploited [23]. When the treatment time was prolonged to 30 min, under strong oxidizing conditions (long irradiation time), the removal efficiencies of AR88 and TOC increased from 50 to 93% and 8 to 10%, respectively.

As shown in Fig. 4, O_3 alone and its combined processes, including UV/O_3, O_3/H_2O_2, and UV/O_3/H_2O_2, all exhibited good performance in AR88 degradation after 5 min and 30 min of treatments. The higher reduction of UV506 achieved can be explained by the AR88 reaction with O_3. It was reported that O_3 directly attacked the unsaturated double bond N=N via electrophilic substitution as the first step [27]. In all O_3-involving experiments, the samples were treated with high doses of O_3 and, as a result, nitrogen-to-nitrogen double bonds (–N=N–) of the azo dye were oxidized and UV506 was reduced. Since the ozone concentration evaluated in this study was much higher than that of •OH, it was expected that O_3 was the main degradation pathway for AR88. Compared with the O_3 system alone, the increased AR88 oxidation in the O_3 combined systems was resulted from the more •OH formation.

Fig. 5 showed that the TOC concentrations decreased from 12.20 mg L^{-1} to 10.94 and 10.71 mg L^{-1} by the O_3 and O_3/H_2O_2 systems after 5 min of treatment, respectively. The TOC removal efficiencies were lower than AR88 degradation efficiencies, indicating an accumulation of intermediates which were resistant to further degradation by O_3. In comparison, •OH radicals could effectively reduce the TOC concentration when the treatment duration was prolonged properly. The higher oxidation potential of •OH radicals than O_3 and its non-selective oxidant property made it more effective in attacking the intermediates from the AR88 degradation. Therefore, as shown in Fig. 5, the combined systems involving O_3 were observed to have a significant increase in TOC removal efficiency when the test durations were prolonged to 30 min. The UV/O_3 and UV/O_3/H_2O_2 systems achieved a reduction of more than 83% of the initial TOC after 30 min of treatment, which might be due to a larger yield of •OH per oxidant. The production yields of •OH in each oxidation process were measured during this study, and the results showed that UV/O_3/H_2O_2 was proved to be the best system for the generation of •OH (Fig. 3). Previous studies also confirmed that the combined system had a higher generation of •OH compared with other advanced oxidation processes [28].

3.3. The variation of pH value in the reaction

The relation between the pH variety and the TOC removal efficiencies was plotted in Fig. 6. It was found that the higher the TOC removal efficiency, the lower the final pH value, which indicated that more short-chain organic acids among the intermediate products were generated. Therefore, the change of pH value in the reaction process might be used as an indication of the mineralization progress [29]. To better illustrate the point, the variety of AR88, TOC, and pH along with treatment time in the UV/H_2O_2/O_3 system was

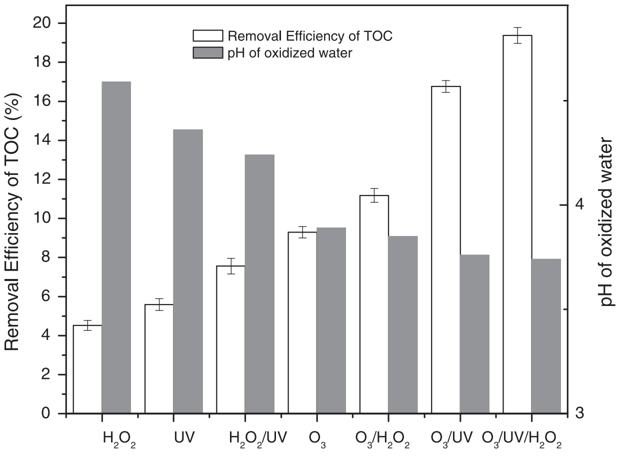

Fig. 6. The relation between the pH variety and the TOC removal (initial AR88 concentration: 25 mg/L; reaction volume: 250 mL; test duration: 5 min; initial pH 6.2; H_2O_2 concentration: 20 mg/L).

plotted in Fig. 7. The results showed that the pH of the AR88 solution decreased rapidly from 6.2 to 3.28 after 5 min and then decreased gradually towards the end of the treatment. The reason is that when the clean air was used as the feeding gas of the ozone generator, strong acids were formed as a consequence of oxidation of nitrogen in air. Besides, Tang et al. [30] also observed that large numbers of NO_x formed from the gas-phase dielectric barrier discharge process because N_2 in air were dissolved in the aqueous phase and subsequently converted to NO_3^- and H^+, resulting in a solution pH decrease when air was used as the feeding gas. Meanwhile, the reduction of AR88 and TOC increased at a rapid rate at the beginning of operation and slow rate afterward. After 30 min, the varieties of pH gradually became a balanced state and the mineralization of AR88 almost completed. Therefore, the pH value could be used as an indication of the mineralization progress in the following studies.

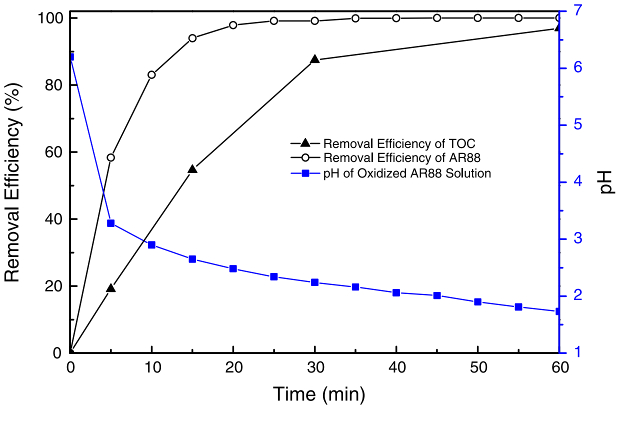

Fig. 7. Variety of AR88, TOC, and pH along with treatment time in the $UV/H_2O_2/O_3$ system (initial AR88 concentration: 25 mg/L; reaction volume: 250 mL; initial pH 6.2; H_2O_2 concentration: 20 mg/L).

3.4. The determination of intermediates

GC-MS analysis was used to identify the possible intermediate products (proposed by using m/z values of the mass spectra) in the degradation process of Acid Red 88 dye. The results showed that the molecular ion peak of AR88 (m/z 400.4) was observed at m/z 376.8, corresponding to the loss of one Na from its structure. In addition, another two prominent peaks at m/z values of 254.9 and 96.8 were observed in the original solution. The peaks at m/z 254.9 and 376.8 particularly diminished as the oxidation time increased. New peaks at m/z values of 61.9, 90.9, 98.8, 107.8, and 146.8 appeared after 1 and 2 min of oxidation, compared with the original sample. After 5 min of treatment, the peaks at m/z values greater than 150 almost disappeared, while the peak at m/z 61.9 showed a marked increase as the major product. The strong and non-specific •OH can react with N=N as well as the C–N bonds and destroy the carbon structure with concomitant formation of intermediates which subsequently undergo further reaction with the formation of lighter molecular weight compounds. The emerging peak at m/z 61.9 suggested the formation of ring opening compounds. In addition, the formation of intermediates such as benzene, naphthalene, naphthalene sulfonic acid, and phthalic acid were confirmed during the degradation and mineralization of AR88.

4. Conclusions

In this work, a series of experiments were performed to study the formation rates of •OH radicals by several oxidation processes, including UV, H_2O_2, O_3, UV/H_2O_2, UV/O_3, H_2O_2/O_3, and $UV/H_2O_2/O_3$ and the degradation and mineralization efficiencies of azo dyes AR88 by various processes were also studied. Furthermore, the pH value of the AR88 solution after the oxidation were determined. In addition, the degradation intermediates were detected by using GC-MS. The conclusions can be drawn as follows:

(1) Single UV, H_2O_2, or O_3 could not generate •OH effectively, while the combined $UV/O_3/H_2O_2$ was proved to be the best system for the generation of •OH among the seven oxidation methods, and the average generation rate of •OH could be up to 1.13 mg L^{-1} min^{-1} in 30 min.

(2) The efficiencies of AR88 degradation and TOC removal closely agreed with the generation rates of •OH in each treatment process. The UV and/or H_2O_2 process showed lower efficiencies of AR88 degradation and mineralization within a short time. However, O_3 alone showed high AR88 degradation efficiency but lower TOC removal compared with the combined systems. The $UV/O_3/H_2O_2$ and UV/O_3 systems were effective in the degradation and mineralization of AR88, and their TOC removal efficiencies were above 83% after 30 min.

(3) The higher the TOC removal rate, the lower the final pH value. The variety of pH value in the reaction process can be used as an indication of the mineralization progress.

(4) The degradation intermediates, including benzene, naphthalene, naphthalene sulfonic acid, and phthalic acid, were detected by GC-MS.

References

[1] J. Madhavan, F. Grieser, M. Ashokkumar, Degradation of orange-G by advanced oxidation processes, Ultrason. Sonochem. 17 (2010) 338–343.
[2] K. Singh, S. Arora, Removal of synthetic textile dyes from wastewaters: A critical review on present treatment technologies, Crit. Rev. Env. Sci. Technol. 41 (2011) 807–878.
[3] K. Golka, S. Kopps, Z.W. Myslak, Carcinogenicity of azo colorants: Influence of solubility and bioavailability, Toxicol. Lett. 151 (2004) 203–210.
[4] M. Bhaskar, A. Gnanamani, R.J. Ganeshjeevan, R. Chandrasekar, S. Sadulla, G. Radhakrishnan, Analyses of carcinogenic aromatic amines released from harmful azo colorants by Streptomyces SP. SS07, J. Chromatogr. A 2003 (1018) 117–123.
[5] N. Mohaghegh, M. Tasviri, E. Rahimi, M.R. Gholami, Nano sized ZnO composites: Preparation, characterization and application as photocatalysts for degradation of AB92 azo dye, Mater. Sci. Semicond. Process. 21 (2014) 167–179.
[6] Z.M. Ni, S.J. Xia, L.G. Wang, F.F. Xing, G.X. Pan, Treatment of methyl orange by calcined layered double hydroxides in aqueous solution: Adsorption property and kinetic studies, J. Colloid Interface Sci. 316 (2007) 284–291.
[7] Y. You, H. Zhao, G.F. Vance, Adsorption of dicamba (3, 6-dichloro-2-methoxy benzoic acid) in aqueous solution by calcined–layered double hydroxide, Appl. Clay Sci. 21 (2002) 217–226.
[8] R. Andreozzi, V. Caprio, A. Insola, R. Marotta, Advanced oxidation processes (AOP) for water purification and recovery, Catal. Today 53 (1999) 51–59.
[9] B. Neppolian, H.C. Choi, S. Sakthivel, Banumathi Arabindoo, V. Murugesan, Solar/UV-induced photocatalytic degradation of three commercial textile dyes, J. Hazard. Mater. 89 (2002) 303–317.
[10] V. Augugliaro, M. Litter, L. Palmisano, J. Soria, The combination of heterogeneous photocatalysis with chemical and physical operations: A tool for improving the photoprocess performance, J. Photochem. Photobiol., C: Photochem. Rev. 7 (2006) 127–144.
[11] M.R. Hoffmann, S.T. Martin, W. Choi, D.W. Bahnemann, Environmental applications of semiconductor photocatalysis, Chem. Rev. 95 (1995) 69–96.
[12] Z. He, L. Lin, S. Song, M. Xia, L. Xu, H. Ying, J. Chen, Mineralization of CI Reactive Blue 19 by ozonation combined with sonolysis: Performance optimization and degradation mechanism, Sep. Purif. Technol. 62 (2008) 376–381.
[13] S.H. Kim, H.H. Ngo, H.K. Shon, S. Vigneswaran, Adsorption and photocatalysis kinetics of herbicide onto titanium oxide and powdered activated carbon, Sep. Purif. Technol. 58 (2008) 335–342.
[14] A. Matilainen, M. Sillanpää, Removal of natural organic matter from drinking water by advanced oxidation processes, Chemosphere 80 (2010) 351–365.
[15] Z. Yang, Z. Yi, X. Jiang, W. Jiang, T.M. Lim, Comparison of the degradation of azo dye AR88 by several oxidation processes, Fresenius Environ. Bull. 22 (2013) 236–241.
[16] T. Chao, J.F. Peng, J.F. Liu, G.B. Jiang, H. Zou, Determination of hydroxyl radicals in advanced oxidation processes with dimethyl sulfoxide trapping and liquid chromatography, Anal. Chim. Acta 527 (2004) 73–80.
[17] Q. Tang, W. Jiang, Y. Zhang, W. Wei, Degradation of azo dye Acid Red 88 by gas phase dielectric barrier discharges, Plasma Chem. Plasma Process. 29 (2009) 291–305.
[18] D.E. Sullivan, J.A. Roth, Kinetics of ozone self-decomposition in aqueous solution, AlChE Symp. Ser. 76 (1980) 142–149.
[19] W.L. Jolly, Modern Inorganic Chemistry, McGraw Hill, New York, NY, 1984, pp. 60–61.
[20] J.H. Baxendale, J.A. Wilson, The photolysis of hydrogen peroxide at high light intensities, Trans. Faraday Soc. 53 (1957) 344–356.
[21] H. Christensen, K. Sehested, H. Corfitzen, Reactions of hydroxyl radicals with hydrogen peroxide at ambient and elevated temperatures, J. Phys. Chem. 86 (1982) 1588–1590.
[22] W.H. Glaze, J.W. Kang, Advanced oxidation processes. Description of a kinetic model for the oxidation of hazardous materials in aqueous media with ozone and hydrogen peroxide in a semibatch reactor, Ind. Eng. Chem. Res. 28 (1989) 1573–1580.
[23] R. Andreozzi, V. Caprio, A. Insola, R. Marotta, Advanced oxidation processes (AOP) for water purification and recovery, Catal. Today 53 (1999) 51–59.
[24] J. Marugán, D. Hufschmidt, M.J. López-Muñoz, V. Selzer, D. Bahnemann, Photonic efficiency for methanol photooxidation and hydroxyl radical generation on silica-supported TiO_2 photocatalysts, Appl. Catal., B 62 (2006) 201–207.
[25] A. Chin, P.R. Bérubé, Removal of disinfection by-product precursors with ozone-UV advanced oxidation process, Water Res. 39 (2005) 2136–2144.
[26] S.R. Sarathy, M. Mohseni, The impact of UV/H_2O_2 advanced oxidation on molecular size distribution of

chromophoric natural organic matter, Environ. Sci. Technol. 41 (2007) 8315–8320.

[27] A. Lopez, H. Benbelkacem, J.S. Pic, H. Debellefontaine, Oxidation pathways for ozonation of azo dyes in a semi-batch reactor: A kinetic parameters approach, Environ. Technol. 25 (2004) 311–321.

[28] C. Gottschalk, J. Libra, A. Saupe, Ozonation of Water and Waste Water, Wiley-VCH, New York, NY, 2000.

[29] W. Zhu, Y. Bin, Z. Li, Z. Jiang, T. Yin, Application of catalytic wet air oxidation for the treatment of H-acid manufacturing process wastewater, Water Res. 36 (2002) 1947–1954.

[30] Q. Tang, W.J. Jiang, Y. Cheng, S. Lin, T.M. Lim, J.R. Xiong, Generation of reactive species by gas-phase dielectric barrier discharges, Ind. Eng. Chem. Res. 50 (2011) 9839–9846.